5-2023

Hydroclimate Effects on Great Salt Lake Decline Since 1980

Siiri Joy Bigalke
Utah State University

HYDROCLIMATE EFFECTS ON GREAT SALT LAKE DECLINE SINCE 1980

by

Siiri J. Bigalke

A thesis submitted in partial fulfillment
of the requirement for the degree

of

MASTER OF SCIENCE

in

Climate Science

_____	_____
Lawrence Hipps, Ph.D.	Nancy Huntly, Ph.D.
Major Professor	Committee Member

_____
Wei Zhang, Ph.D.
Committee Member

UTAH STATE UNIVERSITY
Logan, Utah

2023

ABSTRACT

Hydroclimate effects on Great Salt Lake decline since 1980

by

Siiri Bigalke, Master of Science

Utah State University, 2023

Major Professor: Dr. Lawrence Hipps
Department: Plants, Soils, and Climate

As a terminal basin lake, the Great Salt Lake (GSL) is known to act as a barometer for low frequency climate variability for the Western United States. As thus, there are naturally occurring large changes to GSL elevation levels that vary on time scales from years to decades. However, amongst these naturally occurring interannual changes there has been a significant declining trend in the elevation levels since a string of anomalous pluvial years in the early 1980s. In the summer of 2022, the Great Salt Lake reached its lowest levels in recorded history, which coincided with a two-decades long regional drought in the Western United States. Though climate forcings have been speculated to be a primary source of this decline, the exact contribution and magnitude of drought impacts on the Great Salt Lake decline have been understudied. Analysis here addresses this question by utilizing observational climate records to establish the relationship between precipitation and drought metrics on the GSL elevation levels since

the 1980s, as well as utilizing gridded reanalysis datasets to provide insights into the large-scale atmospheric conditions associated with these regional climate changes. Correlation analysis between streamflow and regional drought metrics reveals that the GSL has become more responsive to drought and less correlated with streamflow. Analyzing atmospheric conditions during the period of record reveals that a strengthened high-pressure system, associated with an intensified upper-level ridging pattern since 1980, has resulted in this pattern of increased aridity. Finally, the future of drought in the GSL watershed is analyzed using a suite of CMIP5 downscaled climate model outputs under two future warming scenarios, of which results indicate that the strongest variable associated with recent GSL decline (annual number of days without precipitable moisture) will increase in the future. Given the GSL's economic and ecological importance, in addition to growing air quality concerns of newly exposed toxic dust from the desiccated lakebed, diagnosing the contributions of regional hydroclimate forcings on the lake's decline is timely. Results from this analysis provides insights into the growing role that drought plays on the GSL's decline and the likelihood of regional drought patterns to intensify in the future.

(43 pages)

PUBLIC ABSTRACT

Hydroclimate effects on Great Salt Lake decline since 1980

Siiri Bigalke

Though the Great Salt Lake naturally varies over time in coherence with regional climate patterns, it has exhibited an overall declining trend since the 1980s and reached its lowest elevation levels on record in the summer of 2022. The changes in the lake level can be separated into two main sets of causes. First, there are the changes in precipitation and evaporation that directly follow the climate properties of the region. Second, there are the changes caused by diversion of water from the major stream flows into the lake. The former follow from nature, while the latter are a direct result of human activities, mainly irrigation. This research aims to analyze the climate impacts on the Great Salt Lake decline by using observed climate data, including precipitation and streamflow records, in addition to constructed drought indices. Results indicate that the regional climate is becoming significantly drier, and that the Great Salt Lake is responding to increases in drought over the changes in precipitation or streamflow. Analysis of future climate model simulations indicated that drought metrics that have been significantly correlated with the Great Salt Lake decline in the past, will intensity in the future depending on the strength of climate warming.

ACKNOWLEDGMENTS

I am deeply grateful to my network of family and friends for their support and encouragement over the last two years. Special thanks as well for the contributions from my committee members, and thanks to Dr. Jon Meyer for the insight on the omega equation, Christine Rumsey for information on USGS streamflow locations, and the many folks who helped me learn about the Great Salt Lake water system.

Siiri Bigalke

LIST OF TABLES

LIST OF FIGURES

Figure Page

CONTENTS

Page

CHAPTER I

INTRODUCTION

The Great Salt Lake (GSL) is the largest saline lake in the western hemisphere and vital to the health of the regional ecosystem and economy of the state of Utah. Though there is significant natural interannual variability of GSL levels, there has been a rapid decline of the water level and areal extent starting in the latter 1980s, after a string of anomalously wet years caused the lake to rise to its second highest levels in recorded history. Since then, it has receded to its current record low reached in the summer of 2022. The decline from the previous record high in 1873 (4,211 feet), to the previous low in 1963 (4,192.2 feet) took 90 years, while the secondary peak in 1987 (4,210.8 feet) to the record low set in 2021 and then again in 2022 occurred within the span of 35 years (Fig. 1b). The rapid rate of this most recent decline (35 years compared to 90 years) coincides with a period of exceptional dry conditions in the long-term record of Utah's climate (Fig. 1a) and is part of a larger two-decade long period of drought in the Western United States (Williams et al., 2022).

While no study to date has documented in detail the role of climate factors in the recent decline of the GSL, a wealth of studies show how interannual changes to the elevation levels are highly respondent to regional climate variability. The GSL is famously known in hydroclimate literature as a 'barometer' for low frequency climate variability (Lall & Mann, 1994). Thanks to its geography as a terminal basin lake, the GSL acts like a giant rain gauge as it integrates hydrological responses to precipitation from the larger Great Basin watershed in the Western United States. Additional studies

about GSL connections with large scale climate variability found that elevation levels vary in coherence with larger atmospheric teleconnection patterns connected with Western Pacific Sea surface temperatures that are related to decadal patterns of regional precipitation (Wang et al., 2010, Wang et al., 2012).

Furthermore, the large drainage area acts as a low pass filter to dampen the effects of high-frequency climate variability on the lake level. Therefore, the GSL lake levels are characterized by cycles at frequencies ranging from interdecadal to interannual time scales, which match those of the inputs to the GSL system, including precipitation, streamflow, and groundwater (Eq. 1). Because the GSL is a terminal basin lake, the only significant way water leaves the system is via evaporation, the rate of which is determined by both climate properties and salinity levels (as salinity is inversely proportional to lake volume, and it reduces evaporation by lowering the water potential of the water).

(Eq. 1) $$\frac{\Delta\, GSL\ Volume}{\Delta\, time} = Precipitation * Surface\ Area + Groundwater + Streamflow - Evaporation * Surface\ Area$$

While the lake levels have been documented to respond strongly to regional climate variability, the natural systems of the Great Salt Lake have also been fundamentally transformed by human interaction. Decades of industrial activity have permanently altered the local landscape, and upstream water diversions of the GSL's

main tributaries for agricultural and urban landscaping use has likely compounded these changes (Wurtsbaugh et al., 2017).

Because the state of Utah does not track yearly water diversion from the GSL tributaries, there is uncertainty about how much the GSL decline can be attributed to water consumption from these water diversions. As the GSL is a high-dimensional system that responds to both human and environmental systems, it is impossible to fully understand the sources of decline without adequate estimates of yearly water diversions from GSL inputs. However, previous sensitivity analysis of the GSL determined that the primary input explaining yearly volumetric changes is the combined streamflow of the Bear River, Jordan River, Weber River, and Davis River with direct precipitation and groundwater playing a smaller role in annual input. Mohammed & Tarboton (2012) found that annual average streamflow input to the GSL from 1950-2010 is about 3 km^3, direct precipitation around 1 km^3, and groundwater ~0.093 km^3 per year.

In summary, the lake level is affected by two sets of processes. First, the climate factors that govern the amount of streamflow into the lake from the source watersheds. Second, the consumptive use of water diverted upstream. The diversion of water does not completely remove inputs to the lake, as some can still return after the diversions, but the water evaporated and transpired into the atmosphere by irrigation after the diversion is lost from the system. Climate also affects the amount of diverted water that is consumed by evapotranspiration from irrigated surfaces and affects the evaporation of water from the lake itself. Thus, climate has both direct and indirect effects on the lake level.

Given the above, it should not be surprising that previous research has demonstrated that the GSL has a very strong relationship with regional climate factors. Hence, it is possible to determine how much the climate could be connected to the recent decline using long-term records of the GSL inputs and outputs. Therefore, the general goal of this research is to document how the rapid decline in lake level since the late 1980s is related to climate factors. Specifically, the objectives are:

1. Examine how four drought related metrics that incorporate precipitation and temperature can explain the elevation decline.
2. Use gridded reanalysis climate data to quantify synoptic weather patterns in the western US correlated with the changes in lake level.
3. Use climate model simulations for two future warming scenarios to quantify how the climate properties that explain lake level will change in the future.

CHAPTER 2

DATA AND METHODS

2.1 Data sources

This study utilizes a suite of observed records, historical reanalysis gridded datasets, and climate model simulations to diagnose the hydroclimate drivers of past Great Salt Lake elevation and to provide insights into future changes in the regional hydroclimate (Table 1). The time series of local hydrologic features, such as the GSL elevation levels and streamflow records of primary tributaries, come from the United State Geological Survey (USGS). While there are multiple GSL elevation records taken at various locations around the lake, the USGS Gauging Station 10010000 at the Saltair Boat Harbor, located on the southern end of the lake, was selected due to its length of record (1895-2021). Six USGS streamflow records for tributaries of the GSL were selected based on the length of record and data consistency. The streamflow records (Table 2) selected include three direct observations for the Bear River ("USGS 10126000 Bear River Near Corinne, UT","USGS 10011500 Bear River Near Utah-Wyoming State Line", "USGS 10118000 Bear River Near Collinston, UT") in addition to a record for the Blacksmith Fork ("USGS 10113500 BLACKSMITH FORK AB UP and L CO.'S DAM NR HYRUM, UT"), which is a tributary of the Bear River. An additional record for the Jordan River ("USGS 10170500 Surplus Canal @ Salt Lake City, UT"), and one for the Weber River ("USGS 1014000 Weber River Near Plain City, UT") were also analyzed. It is important to note that these streamflow records reflect both interannual changes in regional precipitation variability and water diversions for agricultural and industrial

activity. Therefore, multiple records from different tributaries are analyzed in order to increase confidence in the reliability of the streamflow data in use.

Drought metrics used in this analysis come from various gridded data products, including historic in-situ based daily precipitation, the historic Standardized Precipitation Evapotranspiration Index, and simulated precipitation data from 32 Coupled Model Intercomparison Product (CMIP5) models. Historic daily precipitation data for the GSL watershed is taken from the NOAA Climate Prediction Center (CPC) Unified Gauge-Based Analysis of Daily Precipitation which cover the conterminous United States with a 0.25 degree latitude x 0.25 degree longitude grid (Xie et al., 2007). This in situ gauge-based dataset implements optimal interpolation objective analysis technique and is considered more reliable than daily reanalysis counterparts (Alexander et al., 2020). The 1895-2021 Standardized Precipitation Evapotranspiration Index (SPEI) was obtained from the National Integrated Drought Information System (NIDIS) and is calculated from the nClimGrid-Monthly dataset from the Global Historical Climatology Network (GHCN), which is NOAA's primary station data set that integrates climate summaries of land surface stations.

Monthly data for geopotential height at the 500 hPa level (z500) and sea surface temperatures (SSTs) from the ERA5 reanalysis dataset from the European Centre for Medium-Range Weather Forecasts are used to diagnose ocean conditions and the large-scale upper air flow regimes that are typically related with both drought and wet conditions. Monthly 850 hPa zonal wind (*u*, units in m/s) and meridional wind (*v*, units in m/s) from ERA5 is used to identify wind vector anomalies for pluvial and drought years.

500 hPa vertical velocity (ω, units in Pa/s) is also obtained from ERA5 to further describe the vertical motions of the atmosphere, signifying sources or sinks of moisture during pluvial/drought events.

$$\text{(Eq. 2)}\ \left(\nabla^2 + \frac{{f_o}^2}{\sigma}\frac{\partial^2}{\partial p^2}\right)\omega = \frac{f_0}{\sigma}\frac{\partial}{\partial p}\left[\vec{V_g}\cdot\nabla\left(\frac{1}{f_0}\nabla^2\Phi + f\right)\right] + \frac{1}{\sigma}\nabla^2\left[\vec{V_g}\cdot\nabla\left(-\frac{\partial\Phi}{\partial p}\right)\right]$$

Omega (ω) is a partial differential equation that produces estimates of vertical velocity for an isobaric pressure surface (in this application, 500 hPa). It the result of large-scale rotation of the atmosphere and temperature advection. ω represents the 3-D Laplacian of vertical velocity, f is the Coriolis parameter, $\vec{V_g}$is the geostrophic velocity vector, $\Phi$is geopotential, σ is the static stability, and p is atmospheric pressure. The first term on the right-hand of Eq. 2 is known as the differential absolute vorticity advection term and describes the large-scale rotation ("spin") of the atmosphere. The second term on the right-hand side of Eq. 2 is the thermal advection term that describes the large-scale movement of cold or warm air. Because pressure decreases with height, negative values (Fig. 6) indicate upward motion, while positive values of omega indicate downward motion.

2.2 Great Salt Lake watershed averaged data

The GSL watershed (Fig. 1d) is composed of four sub-watersheds that primarily cover northern Utah but extend into southern Idaho, and a small region of eastern Nevada

and western Wyoming. The area is topographically complex with desert landscape to the West and the Wasatch Mountain range dominating the eastern boundary of the watershed. This dramatic elevation gradient represented in the GSL watershed region results in varied climate responses so in order to capture the diverse response of these hydroclimate forcings relevant to GSL variability, a shapefile of the GSL watershed was used on the gridded data to extract data within the extent of its boundary. This watershed level extracted data is averaged into a one-dimensional time series in Fig. 2 and Fig. 3(a, b).

2.3 Hydroclimate metrics

Typical hydrologic metrics usually rely on precipitation or atmospheric moisture "supply" and may not incorporate nor comprehensively characterize the role of evaporation on the state of the local hydroclimate (i.e., atmospheric "demand"). Metrics used in this research are modeled after a newly developed hydroclimate index called the Surplus Deficit Intensity index, which was designed to account for variations in atmospheric "supply" and "demand" forcings but is not explicitly used in this analysis due to its explicit focus on change to hydrological extremes activity (Ficklin, 2019). In this application, two metrics are used to represent the "demand-side", the total number of days without precipitation (hereafter, 'dry days') and the average annual number of consecutive (i.e., more than two) dry days (hereafter, 'dry spell'). These are an estimate of reduction of supply and an indirect estimate of demand, since evaporation is enhanced by days with no precipitation. Surplus intensity, providing the atmospheric "supply-side"

metric, is the average daily precipitation value. These three metrics are calculated for each latitude and longitude grid cell within the GSL watershed boundary in the CONUS CPC daily precipitation data from 1950-2021 and then averaged to obtain the area-averaged time series records in Fig. 3(d, e, f, g).

In addition to the three metrics from the CONUS CPC daily precipitation data, the Standardized Precipitation Evapotranspiration Index (SPEI) calculated from the GHCN nClimGrid-Monthly dataset is used to provide a longer-term record, going back to 1895. SPEI is a recent hydroclimate index designed to provide a more complete approach to quantifying climate change impacts on drought conditions. It has the advantage of treating the role of temperature on drought evolution through incorporating potential evapotranspiration (Beguería et al., 2014). SPEI is used to characterize periods where the average climate has surplus moisture ($SPEI_t$ => $+1\sigma$ $SPEI_{GSL}$), hereafter a ‘pluvial’ period, and those representing a deficit period ($SPEI_t$ = < -1σ $SPEI_{GSL}$), hereafter referred to as a ‘drought’.

CHAPTER 3

RESULTS AND DISCUSSION

3.1 Utah hydroclimate and Great Salt Lake elevation from 1900-2021

The SPEI record for the GSL watershed area reveals that after a period of anomalously wet years in the early 1980s, the overall climate of Northern Utah has trended towards an increasing frequency of drought years, coinciding with the lowest GSL levels in recorded history in 2021/2022. Fig. 1a indicates annual SPEI for the area within the Great Salt Lake watershed region depicted in Fig. 1d from 1900-2021. The direction of elevation change (Fig. 1c) reflects the average annual state of the regional hydroclimate, as described by the SPEI index. Though there are exceptions in the record, $+SPEI_t$ coincides with positive $+\Delta GSL_t$ and $-SPEI_t$ with $-\Delta GSL_t$. From this broad overview of the annual state of the climate and resulting changes in interannual variability, several key events in the record stand out. The pluvial event from (roughly) 1980-1984 is evident in terms of its sheer magnitude (more than $> 2\sigma$ $SPEI_{GSL}$) and the resulting increases in annual tendency. Though this period has been studied, the atmospheric conditions causing this high precipitation activity are still unknown (Karl & Young, 1986). Since this anomalous pluvial period in the early 1980s, drought-like conditions have dominated the local hydroclimate, and the GSL elevation levels have declined to their lowest values on record. The number of pluvial events (n = 7) since 1980 have occurred half as frequently as drought events (n = 14).

3.2 GSL watershed averaged hydroclimate trends and correlations with GSL elevation

According to the water budget equation for the Great Salt Lake (Eq. 1), the inputs into this closed system come from streamflow, direct precipitation onto the lake, and groundwater. Because the GSL is a terminal basin lake, with no outlet tributaries, the only way water leaves this closed system is through evaporation. By analyzing trend in the hydroclimate variables dry days, dry spell, surplus intensity, and the SPEI index, the relative contribution of the recent decline from the inputs and outputs of this system are examined from a climate perspective.

The watershed-averaged time series of dry days and dry spell reveal greater spatial agreement with drought-related metrics, dry days and dry spell, than with the metric for capturing input changes, surplus intensity (Fig. 2a-d). The high elevation eastern boundary of the GSL watershed, which includes the Bear River and Wasatch Mountain range, shows a general drying trend from 1980-2021. However, a more complicated picture emerges regarding changes to daily precipitation values, with significant areas of both increasing and decreasing trends along the eastern GSL watershed boundary. SPEI shows the greatest spatial agreement, with widespread significant reductions from 1980-2021 (Fig 2d).

Because previous analysis has established that the GSL elevation levels have a significant lagged relationship with regional hydroclimate patterns due to the remote teleconnection of Western US precipitation patterns forced by the Quasi-Decadal Oscillation pattern of Pacific sea surface temperatures (Wang et al., 2010; Wang et al., 2012), correlations between the various GSL watershed-averaged hydroclimate metrics and the GSL levels are tested by lagging the GSL elevation back by up to 6 years from

the time series of hydroclimate metrics. Fig. 3a shows that the correlations between annual detrended GSL elevation and detrended GSL hydroclimate metrics from 1980-2021 peak at the lag years 3 and 4, in agreement with previous findings (Wang et al., 2010). The strongest correlations for this time period occur at the lag year 3 and 4 for surplus intensity and SPEI indices, and similarly dry spell and dry days have significant, though slightly weaker, correlations at the lag year 3 level for the period of 1980-2021. This lag accounts for the delay in water received as precipitation in the large source area eventually finding its way into the lake and changing its volume.

In order to test how the strength of the relationship between GSL elevation and the GSL watershed hydroclimate metrics has changed over time, 30-year rolling averages from 1950-2021 are applied with the 3-year lagged GSL elevation (Fig. 3b). With the GSL elevation lag of 3-years (hereafter, GSL-3) resulting in the strongest correlations in both of the "demand-side" metrics (dry days, and dry spell), the "supply-side" metrics (surplus intensity), and the blended metric (SPEI), it is used for these 30-year rolling average correlations. Fig 3b shows that since the anomalous pluvial period in the early 1980s, the "demand" hydroclimate metrics (particularly dry days) have stayed more consistently and highly correlated with GSL-3, compared to the "supply metrics". Since the 1980s, the GSL-3 30-year rolling correlations with surplus intensity (which closely follows SPEI) have maintained significance, but the coefficient's values exhibit a downward trend since the early 2000s, almost surpassing the threshold for statistical insignificance (dashed line in Fig. 3b), though it recovers slightly by the end of the record. In contrast, dry days and dry spell yield more stable coefficient values, and

largely grow in strength from the 1980s until the end of the record. The dry days metric yields a particularly strong correlation coefficient value of nearly -0.8 at the end of the record.

To get additional perspective on how streamflow (the primary input into the GSL) might contribute to GSL decline, the 30-year rolling correlations of GSL-3 are also applied to six USGS streamflow records of tributaries into the GSL (including the Bear River, Jordan River, Weber River, and the Blacksmith Fork River which is a tributary into the Bear River) (Fig. 3c). All six records exhibit similar 30-year averaged correlation patterns similar to the surplus intensity record, with significant declines in coefficient values in the early 2000s which reach their lowest levels near present day. The combined results of Fig. 3b and 3c indicate that GSL levels have become more responsive to "demand" metrics since the 1980s while "supply" metrics and streamflow has become less correlated with GSL levels during this same time period, suggesting that drought is playing a greater role in the interannual variability of GSL levels than at any other time in the lake's recorded history.

3.3 Synoptic changes associated with GSL decline

Analysis outlined in 3.1 revealed that drought events after 1980 (n=14) have occurred twice as much as drought events before 1980 (n=7), in addition to occurring twice as frequent than pluvial events from 1980-2021 (n=7). The increasing occurrence of drought years compared to pluvial events indicates a hydroclimate characterized by lack of moisture availability since the 1980s, which is further supported by findings in section

3.2 showing that lagged GSL levels are becoming more correlated to drought metrics than precipitation or streamflow. To understand the atmospheric drivers of increased drought activity associated GSL decline since the 1980s, 500 hPa geopotential height anomalies (z500, Fig. 4), sea surface temperatures anomalies (SSTs, Fig. 5) and 500 hPa vertical velocity (Fig. 6) are composited for pluvial and drought years for the period 1950-1979 and 1980-2021. As atmospheric circulation regimes exhibit significant seasonal variation, both winter (NDJFM, left column) and summer (JJA, middle column) composites in addition to the annual composites (right column) of atmospheric variables are shown in Fig. 4 and 5.

Composites of the summertime z500 (anomalies calculated from 1980-2021 averaged conditions) reveal that atmospheric circulation during pluvial years is associated with lower geopotential heights, with a strong anomalous trough concentrated over the Pacific Northwest in the period before 1980 (Fig. 4a, middle column). Interestingly pluvial winter composites exhibit lower pressure anomalies in this same region after 1980 (probably because this time period includes the numerous extreme wet years in the early 1980s). Drought years are associated with an atmospheric circulation pattern of an elongated high pressure ridge system from the Western United States to the Northeast Atlantic coast during the winter after 1980. The combined results of the seasonal z500 composites in Fig. 4 indicate that drought years are dominated by high pressure upwind of Utah after 1980, while post 1980 changes for pluvial years are mixed, with a lower pressure system off the Western US for composited pluvial winters, but a higher anomalous pressure system during pluvial summers. Pacific Ocean temperature change is

considered as a large source of predictability for Western US precipitation variability, and therefore possible SSTs shifts before and after 1980s associated with GSL decline are also examined. The drought event changes are fairly consistent across both seasons before and after 1980 (Fig. 5b); overall SSTs are warmer after 1980 except a small area of the central pacific which exhibits slight cooling. Similarly, SSTs are warmer during pluvial events, with noticeable warming centered off the Western coast of South America and extending into the central tropical Pacific, and anomalous cooling in the North-Central Pacific region.

Fig. 6 shows the composites of 500 hPa vertical velocity and 850 hPa wind vector anomalies for pluvial and drought years before and after 1980 (seasonal changes omitted for simplicity). Of significance in this figure is the intensified anticyclonic circulation pattern during drought years after 1980 off the Pacific Northwest coast (right column, middle panel), which would be associated with negative shear vorticity on the downstream side of this upper-level ridge, preventing moisture transport to the Western US region. This ridging pattern in the 850 hPa wind vector anomalies for drought years after 1980 matches results of the upper-level dynamics revealing anomalous high pressure (z500 anomalies in Fig. 4b of composited drought events). While the 850 hPa wind vector anomalies reveal near surface anomalous anti-cyclonic activity, the 500 hPa vertical velocity is used to investigate mid-atmospheric conditions analysis in Fig. 6. Recall that negative values of omega (blue) indicate upward motion as rising air indicating sources of moisture while positive values (red) of omega indicate downward motion indicating sinking air motion associated with moisture depletion. Results of

composited vertical velocity in Fig. 6 also shows the Pacific Northwest to have strengthened downward vertical velocity after 1980 in both the Pluvial and Drought year events, though considerably stronger for Drought years.

The higher frequency of high-pressure system associated with drought years over the low pressure dominated circulatory patterns of pluvial anomalies reflects research showing that troughing activity has decreased in frequency in the Western US since 1980 while the heat-trapped ridge systems exhibit no change in trend (Zhang et al., 2021). Furthermore, other research incorporating paleo records has put this recent drying trend in a multi-century context, showing that 2000-2021 was the driest two-decade period in the American Southwest since 800 CE (Williams et al., 2020; Williams et al., 2022). Both Zhang et al., 2021 and Williams et al., 2020 used climate model output to reveal significant contributions of anthropogenic forcing on recent western north America drying trend.

3.4 Future trends in GSL watershed area drought

While results from Fig. 1 and 2 reveal that regional climate of the GSL is drying, and Fig. 3 indicates that the GSL elevation is becoming more correlated with drought, the likelihood of future drought changes cannot be determined based on these observations. Therefore, to understand how climate variables that are significantly correlated with GSL levels will changes in the future, 32 CMIP5 climate models are analyzed. With the lagged hydroclimate metrics exhibiting strong correlations with GSL elevation levels (particularly the drought metrics dry days and dry spell in Fig. 3b), the future trends for

CPC-based hydroclimate metrics (dry days, dry spell, and surplus intensity) are analyzed in these CMIP5 models (Fig. 7a-c).

End of century changes to dry days, dry spell, and average daily are dependent on the degree of warming by end of century, though all metrics appear to exhibit an increasing trend though the changes to dry spell length and daily precipitation are considerably weaker than changes to dry days. If the significant negative relationship between dry days and GSL elevation changes over the last four decades continues it is possible that future elevation levels will exhibit a decline in response to increases in dry days. However, this analysis alone cannot provide physical justification that this trend will continue in the future, as the simulations come from climate models. Regardless, future climate model outputs indicate that the strongest variable associated with recent GSL decline (annual number of days without precipitable moisture) will increase in the future, provides meaningful insights that can assist in adaptation purposes.

CHAPTER 4

CONCLUSION

The Great Salt Lake is a high dimensional system that is historically influenced by regional climate forcings but has become more affected by human activity over the last century. Certain variables, particularly streamflow, have been heavily impacted by agricultural and residential water use. The degree to which reductions in annual streamflow are the result of anthropogenic or natural causes is unclear because local climate factors also likely drive decision making processes of farmers and other local water use stakeholders (i.e., low precipitation years could cause farmers to withdraw more water from streamflow tributaries, thus compounding already low streamflow rates during a drought year). The lack of local and regional information about withdrawals is not unique to Northern Utah and is a challenge across the Western United States (Schumacher et al., 2022). Improvements to irrigation use information (in this case from streamflow diversions) would provide even more insights into the anthropogenic versus climate factor responsible for the declining GSL elevation levels.

However, the role of climate in the changes in GSL volume can be estimated with the suite of data that are available, which is what this research attempted to do by utilizing direct observations and state of the art reanalysis climate products. Results indicate that the regional climate has trended towards an increasing frequency of drought years since 1980, due to intensified atmospheric ridging patterns off the coast of the Western US. As a result, the GSL has become more responsive to drought metrics since the 1980s while precipitation rates and streamflow have become less correlated with GSL levels during

this same time. Climate model output indicates that drought metrics which have been becoming more strongly correlated with GSL levels, will increase in the future. This would suggest that in the long-term the lake level although experiencing fluctuations, will generally continue to decline. While these results are useful for a general level of understanding of the recent changes in lake level, more processes need to be quantified such as the changes in consumptive water use of diverted water and actual evaporation by the lake itself and its response to climate variations. These would help to improve physically based modeling efforts to provide more definitive insights into GSL changes.

REFERENCES

Alexander, L. V., Bador, M., Roca, R., Contractor, S., Donat, M. G., & Nguyen, P. L. (2020). Intercomparison of annual precipitation indices and extremes over global land areas from in situ, space-based and reanalysis products. *Environmental Research Letters*, *15*(5), 055002.

Beguería, S., Vicente-Serrano, S. M., Reig, F., & Latorre, B. (2014). Standardized precipitation evapotranspiration index (SPEI) revisited: parameter fitting, evapotranspiration models, tools, datasets and drought monitoring. *International journal of climatology*, *34*(10), 3001-3023.

Ficklin, D. L., Abatzoglou, J. T., & Novick, K. A. (2019). A new perspective on terrestrial hydrologic intensity that incorporates atmospheric water demand. *Geophysical Research Letters*, *46*(14), 8114-8124.

Karl, T. R., & Young, P. J. (1986). Recent heavy precipitation in the vicinity of the Great Salt Lake: just how unusual?. Journal of Applied Meteorology and Climatology, 25(3), 353-363

Lall, U., & Mann, M. (1995). The Great Salt Lake: A barometer of low-frequency climatic variability. *Water Resources Research*, *31*(10), 2503-2515.

Mohammed, I. N., & Tarboton, D. G. (2012). An examination of the sensitivity of the Great Salt Lake to changes in inputs. *Water Resources Research*, *48*(11).

Schumacher, B. L., Yost, M. A., Burchfield, E. K., & Allen, N. (2022). Water in the West: Trends, production efficiency, and a call for open data. *Journal of Environmental Management*, *306*, 114330.

Wang, S. Y., Gillies, R. R., Jin, J., & Hipps, L. E. (2010). Coherence between the Great Salt Lake level and the Pacific quasi-decadal oscillation. *Journal of Climate*, *23*(8), 2161-2177.

Wang, S. Y., Gillies, R. R., & Reichler, T. (2012). Multidecadal drought cycles in the Great Basin recorded by the Great Salt Lake: Modulation from a transition-phase teleconnection. *Journal of Climate*, *25*(5), 1711-1721.

Williams, A. P., Cook, E. R., Smerdon, J. E., Cook, B. I., Abatzoglou, J. T., Bolles, K., Baek, S.H., Badger, A.M. & Livneh, B. (2020). Large contribution from anthropogenic warming to an emerging North American megadrought. *Science*, *368*(6488), 314-318.

Williams, A. P., Cook, B. I., & Smerdon, J. E. (2022). Rapid intensification of the emerging southwestern North American megadrought in 2020–2021. *Nature Climate Change*, *12*(3), 232-234.

Wurtsbaugh, W. A., Miller, C., Null, S. E., DeRose, R. J., Wilcock, P., Hahnenberger, M., Howe, F., & Moore, J. (2017). Decline of the world's saline lakes. *Nature Geoscience*, *10*(11), 816-821.

Xie, P., A. Yatagai, M. Chen, T. Hayasaka, Y. Fukushima, C. Liu, and S. Yang. (2007). A gauge-based analysis of daily precipitation over East Asia, J. Hydrometeorol., 8, 607. 626.

Zhang, W., Hari, V., S-Y Wang, S., LaPlante, M. D., Garfin, G., Affram, G., & Kumar, R. (2022). Fewer troughs, not more ridges, have led to a drying trend in the western United States. *Geophysical Research Letters*, *49*(1), e2021GL097089.

FIGURES

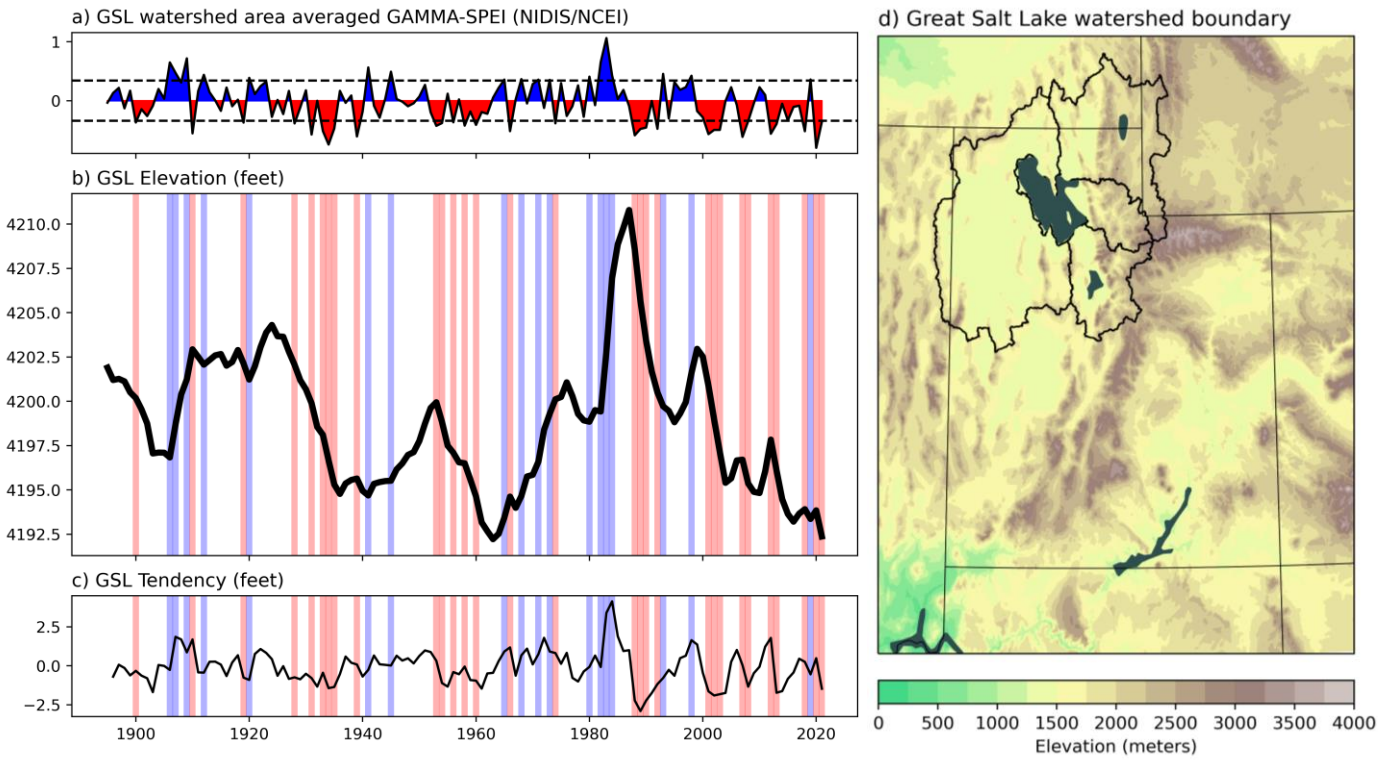

Figure 1. (a) Time series of average annual Standardized Precipitation Evaporation Index (SPEI) values averaged for the Great Salt Lake watershed boundary (d) with dashed line indicates values above and below one standard deviation. (b) Annual Great Salt Lake elevation levels in feet, recorded at (USGS Gaging Station 10010000 at the Saltair Boat Harbor) from 1900 – 2021 and (c) average annual elevation tendency. Solid blue and red bars in (b) and (c) represent years where SPEI values are one standard deviation above the mean (blue), known as a 'pluvial' year, and one standard deviation below the mean (red), indicating a 'drought' year. (e) and (f) show composites of the 500 hPa geopotential height anomalies for the summer months (JJA) for pluvial years (n = 7) and drought years (n =14) since 1980.

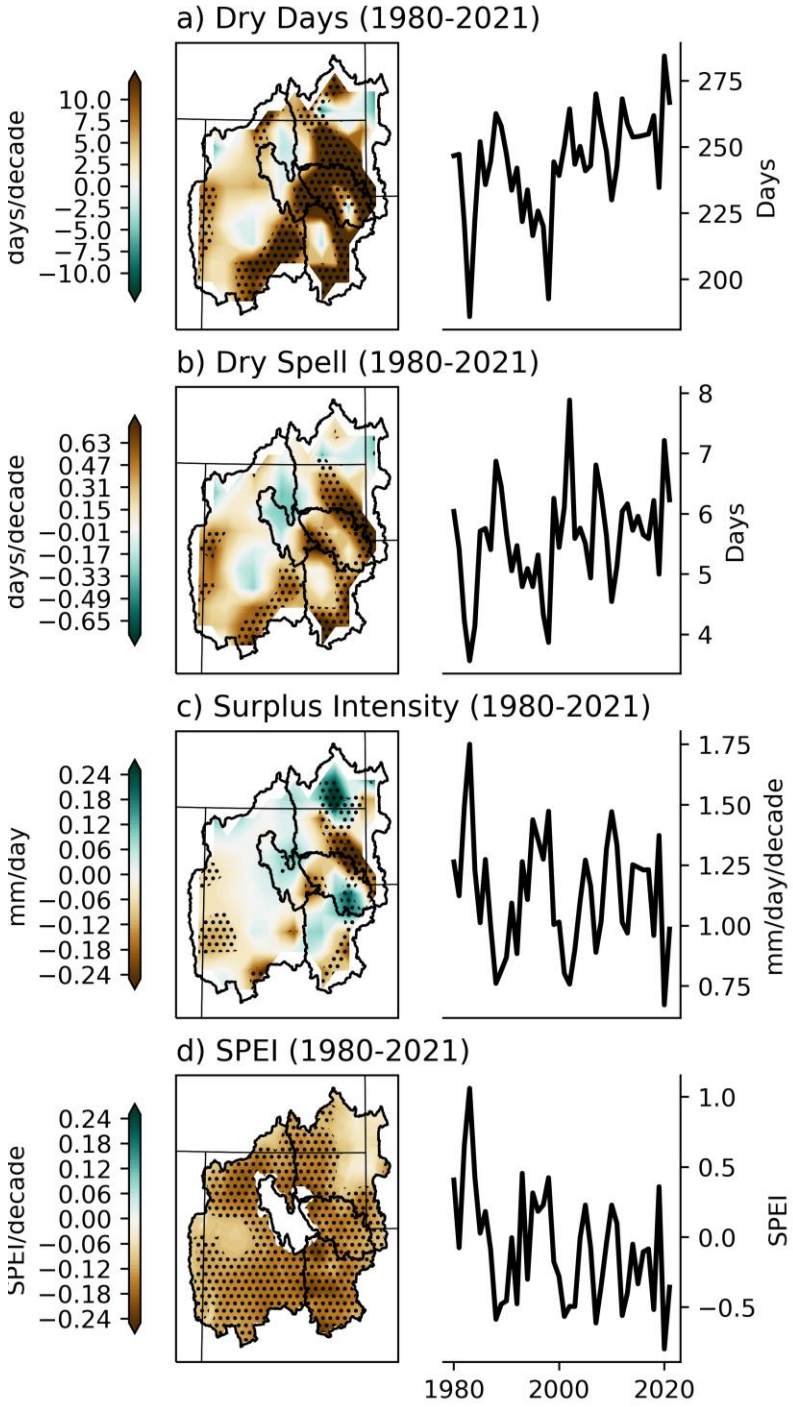

Figure 2. GSL watershed spatial trend (left column) and GSL watershed averaged time series (right column) of hydroclimate variables **a)** dry days, **b)** dry spell, **c)** surplus intensity, and **d)** SPEI from 1980-2021. Stippling in spatial trend figures denotes significance at $p < 0.05$ level.

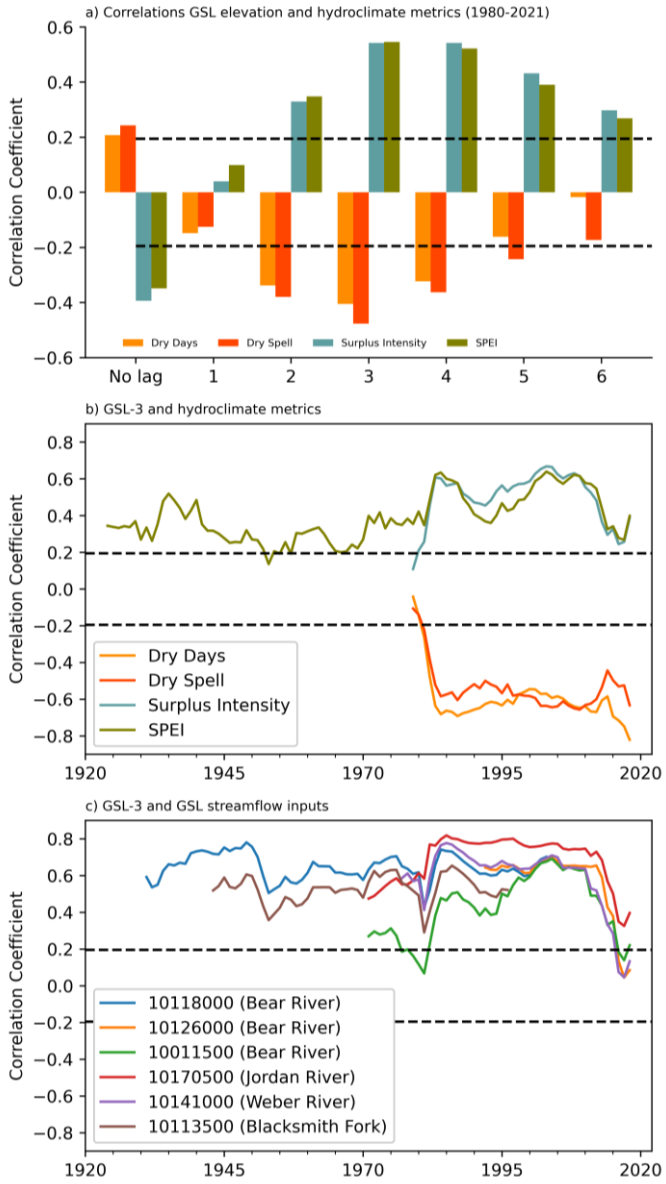

Figure 3. a) Correlations of detrended hydroclimate metrics including dry days (orange), dry spell (red), surplus intensity (blue), and SPEI (green) with detrended GSL elevation data from 1980-2021 with GSL elevation lagged up to six years behind each hydroclimate metric. **b)** 30 year rolling correlations between the 3-year lagged GSL elevation and hydroclimate metrics. SPEI 30 year rolling correlations from 1900-2021 and dry days, dry spell, and surplus intensity from 1950-2021. **c)** 30 year rolling correlations between the 3-year lagged GSL elevation and streamflow records of primary tributaries into the GSL, including the Bear River, Jordan River, Weber River, and Blacksmith Fork. Dashed line represent significance at $p < 0.05$ in a-c.

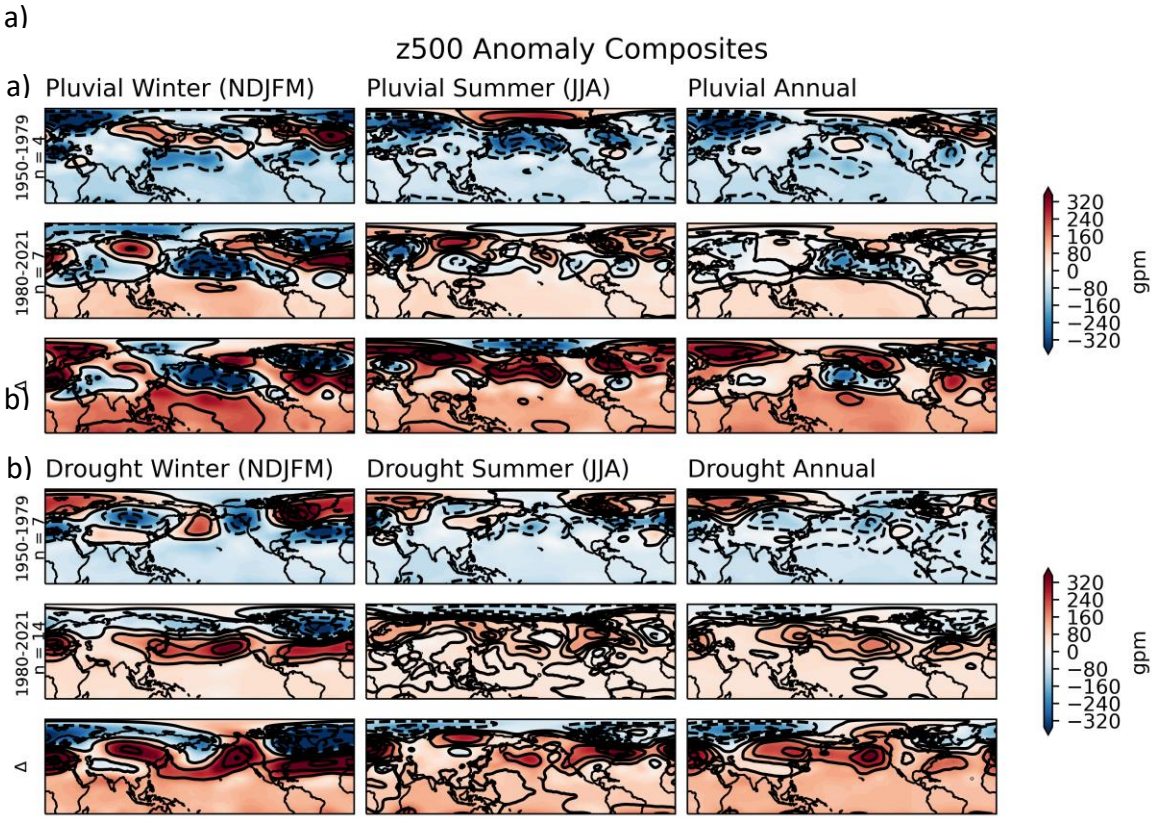

Figure 4. Composites of z500 anomalies for pluvial years (**a**) and drought years (**b**) for events from 1950-1979 (top panel), 1980-2021 (middle panel) and the difference (row 2–row 1).

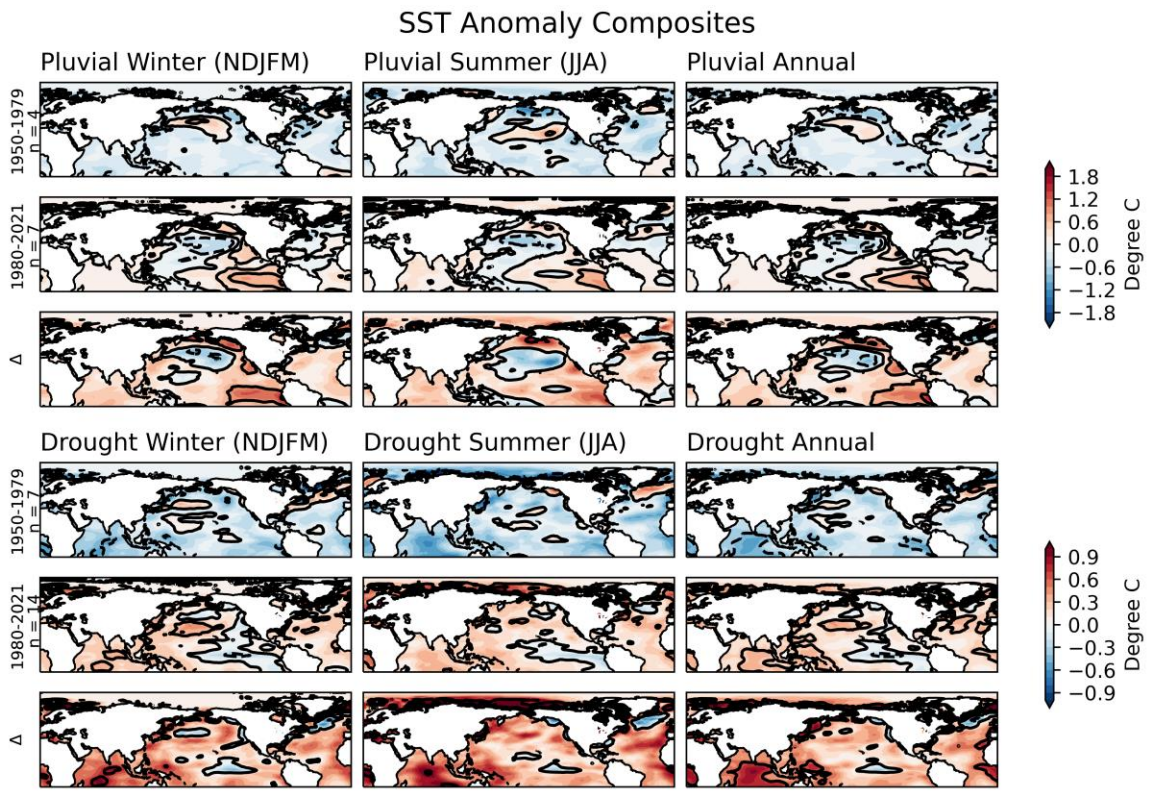

Figure 5. Composites of sea surface temperature anomalies for pluvial years (**a**) and drought years (**b**) for events from 1950-1979 (top panel), 1980-2021 (middle panel) and the difference (row 2– row 1).

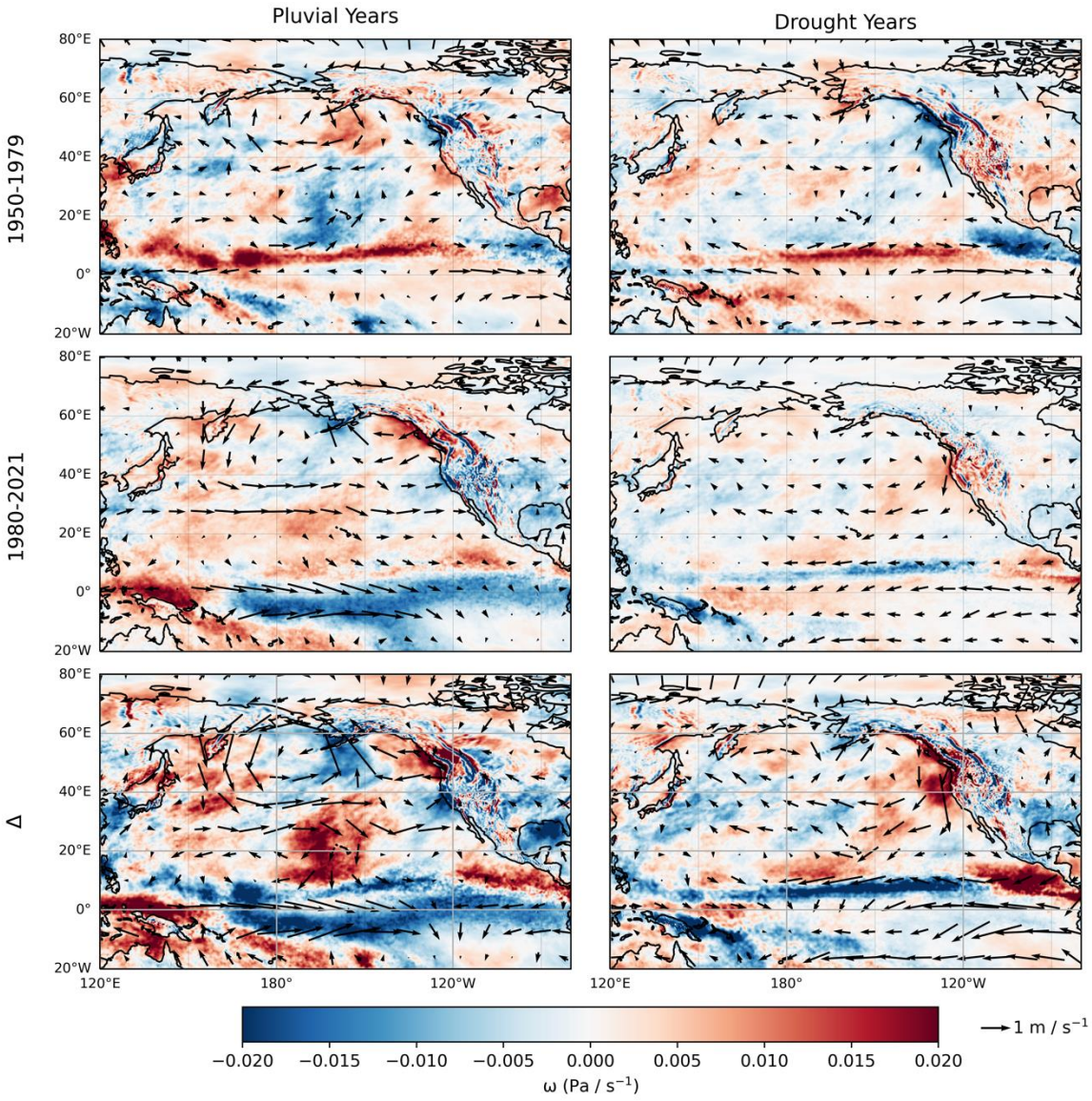

Figure 6. Composites of 500 hPa vertical velocity (ω) and 850 hPa wind vectors anomalies for pluvial years (left column) and drought years (right column) from 1950-1979 (first row) and 1980-2021 (second row). Third row shows the difference between the two periods (row 2 – row 1). Anomalies calculated from full period average (1950-2021).

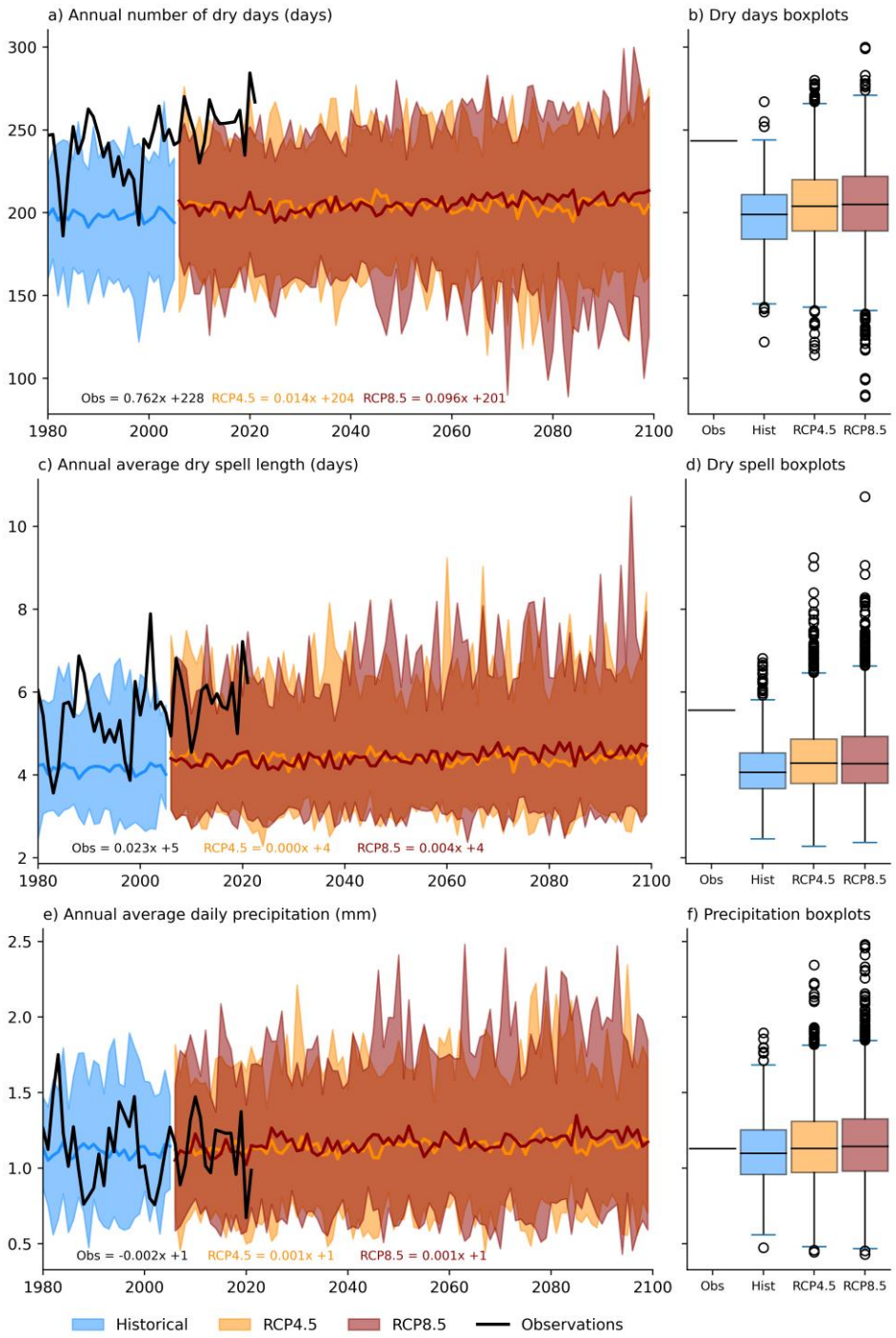

Figure 7. Past and future trends in drought metrics using CONUS downscaled 32 CMIP5. Time series of the sum of annual days without precipitation from 1980 to 2099 **(a-b)**, annual average dry spell length (**c-d**), and average daily precipitation (**e-f**). The black line is the observational data from the GSL watershed averaged data from CPC from 1980-2021 and solid blue line is the average of the historical runs (1980-2005) of

the 32 CMIP5 models with the spread representing the maximum and minimum number of annual dry days from the 32 models while the orange line is the model average for the RCP4.5 future data (2006-2099), and red line and spread representing the RCP8.5 scenario data (2006-2099). (b, d, and f) summarize the spread of annual dry days, dry spell, and daily precipitation, for the observed data (black box), and historical and RCP4.5 and RCP8.5 CMIP5 downscaled data (blue, orange and red boxes) of all years in all 32 CMIP5 models. The boxes extend from the 1st quartile to the 3rd quartile values, with line at the median (Q2). Data beyond 1.5 * (Q3 – Q1) are considered outliers and represented by open circles.

TABLES

Table 1: Data variables & sources

Variable	Dataset	Source	Time	Resolution
Great Salt Lake elevation at Saltair boat harbor	USGS Gauging Station 10010000	United States Geological Survey (USGS)	1895-2021	n/a
Streamflow records	Various (see Table 2)	USGS	Varies (see Table 2)	n/a
Observed Daily Precipitation	CPC Daily Gauge Based Precipitation	NOAA Climate Prediction Center	1950-2021	0.25° x 0.25°
U.S. Monthly Standardized Precipitation Evapotranspiration Index (SPEI)	Derived from nClimGrid	Global Historical Climatology Network/NIDIS	1895-2021	~0.04° x ~0.04° (5x5 km)
500 hPa geopotential height (z500)	ERA5	European Center for Medium-Range Weather Forecasts (ECMWF)	1950-2021	0.25° x 0.25°
Sea surface temperatures (SST)	ERA5	European Center for Medium-Range Weather Forecasts (ECMWF)	1950-2021	0.25° x 0.25°
850 hPa U-wind (u)	ERA5	ECMWF	1950-2021	0.25° x 0.25°
850 hPa V-wind (v)	ERA5	ECMWF	1950-2021	0.25° x 0.25°
500 hPa Vertical Velocity (ω)	ERA5	ECMWF	1950-2021	0.25° x 0.25°
Downscaled CONUS Daily precipitation	CMIP5 downscaled	32 global climate modeling	1980-2005 2006-2099	0.0625° x 0.0625°

	project for CONUS	centers (Table 3)		(1/16° x 1/16°)

Table 2: USGS Streamflow records

Number	Name	Time	Latitude	Longitude	Notes on Location
10126000	BEAR RIVER NEAR CORINNE, UT	1949-2021	41.57	-112.10	Location near the terminus of the Bear River where it empties into the GSL. Also near the GSL Migratory Bird Refuge.
10118000	BEAR RIVER NEAR COLLINSTON, UT	1902-2006	41.83	-112.05	Site located downstream of Cutler Reservoir, slightly further upstream than 10126000.
10011500	BEAR RIVER NEAR UTAH-WYOMING STATE LINE	1942-2021	40.96	-110.85	Located on north side of the Uinta mountains, just outside of Wasatch National Forest.
10170500	SURPLUS CANAL @ SALT LAKE CITY, UT	1942-2021	40.72	-111.92	Surplus canal of the Jordan River, located in Salt Lake City.
10140000	OGDEN RIVER BELOW PINEVIEW DAM NEAR OGDEN, UTAH	1948-2021	41.25	-111.84	Site located on Ogden River, below the Pineview reservoir in the Cache National Forest. (Feeds into Weber River).
10113500	BLACKSMITH FORK AB UP and L CO.'S DAM NR HYRUM, UT	1914-2021	41.62	-111.73	Site located on the Blacksmith Fork (a tributary of the Bear River) in the Cache National Forest.

.

Table 3: CMIP5 Models

Model	Institute ID	Resolution	Ensemble Size
ACCESS1-0	CSIRO-BOM	1/16° lat x lon (~ 6 km by 6 km)	1
ACCESS1-3	CSIRO-BOM	1/16° lat x lon	1
bcc-csm1-1	BCC	1/16° lat x lon	1
bcc-csm1-1-m	BCC	1/16° lat x lon	1
CanESM2	CCCMA	1/16° lat x lon	1
CCSM4	NCAR	1/16° lat x lon	1
CESM1-BGC	NCAR	1/16° lat x lon	1
CESM1-CAM5	NCAR	1/16° lat x lon	1
CMCC-CM	CMCC	1/16° lat x lon	1
CMCC-CMS	CMCC	1/16° lat x lon	1
CNRM-CM5	CNRM-CERFACS	1/16° lat x lon	1
CSIRO-Mk3-6-0	CSIRO-QCCCE	1/16° lat x lon	1
EC-EARTH	ICHEC	1/16° lat x lon	1
FGOALS-g2	LASG-CESS	1/16° lat x lon	1
GFDL-CM3	NOAA-GFDL	1/16° lat x lon	1
GFDL-ESM2G	NOAA-GFDL	1/16° lat x lon	1
GFDL-ESM2M	NOAA-GFDL	1/16° lat x lon	1
GISS-E2-H	NASA-GISS	1/16° lat x lon	1
GISS-E2-R	NASA-GISS	1/16° lat x lon	1
HadGEM2-AO	NIMR-KMA	1/16° lat x lon	1
HadGEM2-CC	MOHC	1/16° lat x lon	1
HadGEM2-ES	MOHC	1/16° lat x lon	1
inmcm4	INM	1/16° lat x lon	1
IPSL-CM5A-LR	IPSL	1/16° lat x lon	1
IPSL-CM5A-MR	IPSL	1/16° lat x lon	1
MIROC5	MIROC	1/16° lat x lon	1

MIROC-ESM	MIROC	1/16° lat x lon	1
MIROC-ESM-CHEM	MIROC	1/16° lat x lon	1
MPI-ESM-LR	MPI-M	1/16° lat x lon	1
MPI-ESM-MR	MPI-M	1/16° lat x lon	1
MRI-CGCM3	MRI	1/16° lat x lon	1
NorESM1-M	MRI	1/16° lat x lon	1